ACS APPLIED MATERIALS & INTERFACES

Research Article

www.acsami.org

Copper Nanowires as Conductive Ink for Low-Cost Draw-On Electronics

Naveen Noah Jason,[†] Wei Shen,[†] and Wenlong Cheng*[,†,‡]

[†]Department of Chemical Engineering, Monash University, Clayton, Victoria 3800, Australia

[‡]Melbourne Centre for Nanofabrication, 151 Wellington Road, Clayton, Victoria 3168, Australia

Supporting Information

ABSTRACT: This work tackles the complicated problem of clump formation and entanglement of high aspect ratio copper nanowires, due to which a well dispersed solution for use as a true ink for drawable electronics has not been made until now. Through rheology studies even a hard to use material like copper nanowires was tailored to be made into a highly efficient conductive ink with only 2 vol % or 18.28 wt % loading which is far lower than existing nanoparticle based inks. This versatile ink can be applied onto various substrates such as paper, PET, PDMS and latex. By using the ink in a roller ball pen, a bending sensor device was simply drawn on paper, which demonstrated detection of various degrees of convex bending and was highly durable as shown in the 10 000 bending cycling test. A highly sensitive strain sensor which has a maximum gauge factor of 54.38 was also fabricated by simply painting the ink onto latex rubber strip using a paintbrush. Finally a complex conductive pattern depicting the Sydney Opera House was painted on paper to demonstrate the versatility and robustness of the ink. The use of Cu NWs is highly economical in terms of the conductive filler loading in the ink and the cost of copper itself as compared to other metal NPs, CNT, and graphene-based inks. The demonstrated e-ink, devices, and facile device fabrication methods push the field one step closer to truly creating cheap and highly reliable skin like devices "on the fly".

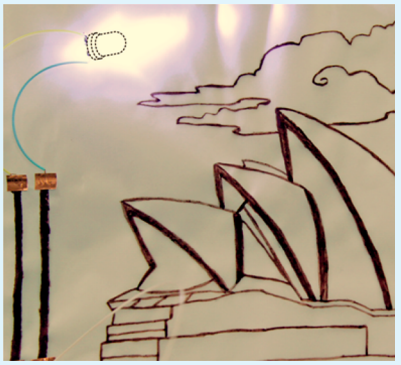

KEYWORDS: *copper nanowires, conductive ink, draw-on electronics, strain sensor, bending sensor*

INTRODUCTION

Drawable electronics can offer a number of benefits compared to conventional rigid circuit board technologies, such as facile low-cost and large-area fabrication on various flexible substrates. Toward this goal, various strategies ranging from laboratory scale methods such as vacuum filtration-membrane transfer,[1−3] meyer rod coating,[4−6] doctor blading,[7,8] and drop casting[9,10] to potentially industry scalable methods such as inkjet printing,[11−14] electrospinning,[15−17] and dip coating[18,19] have been developed. Of all these methods the pen-on-paper strategy emerges to be a facile ink delivery method for large area patterning on variety of substrates. In particular, the recent success in pen-on-paper approach[20,21] has shown that it is possible to deliver functional electrically conductive patterns onto various substrates for applications in chemical,[22] biosensor,[23] SERS,[24] and motion sensors.[25] Some recent reports have further advanced this concept and developed the pencil-on-paper strategy for cheap electronics.[26−28]

Central to all the aforementioned approaches is an electrically conductive ink, which is a complex system governed by various properties, such as surface tension, viscosity, humidity, substrate binding ability, etc.[29] Substantial research efforts have been devoted to nanomaterials for formulating such electronic inks, including metallic nanoparticles,[11,20,21,30] graphene,[31] and carbon nanotubes (CNTs).[32,33] To date, noble-metal-based nanoparticle solutions have dominated the printed electronics industry due to their facile synthesis and chemical stability under ambient conditions. Majority of the electrically conductive inks reported in earlier works utilize zero dimensional sphere or sphere-like nanoparticles (NPs) as their constituents.[11,20,21,30] In principle, electronic inks from one-dimensional metal nanowires are ideal because they can substantially enhance percolation conductivity[34,35] yet lower materials consumption. However, limited success has been achieved for one-dimensional nanowires because of complex problems, such as entanglement of fibers, the clogging of printing nozzles and nibs, and a nonlinear viscosity profile, which is the signature of a suspension with high aspect ratio particles. Thus, it is desired to develop electronic inks from 1D metal nanowires, ideally from earth-abundant materials, such as copper.

EXPERIMENTAL SECTION

Materials. Hexadecylamine (HDA) Sigma-Aldrich, copper chloride ($CuCl_2 \cdot 2H_2O$) Sigma-Aldrich, D-glucose (α or β) Merck, hydroxypropyl cellulose (HPC) Sigma-Aldrich, 20 mesh, M_w = 1 000 000.

Cu NWs Synthesis. Our Cu NWs were synthesized using a scaled up amine-capped and glucose-based reduction method.[49] An oil bath was preheated to 100 °C, into which a screw cap borosilicate bottle with 50 mL of water, was immersed. When bubbles began to appear in

Received: May 25, 2015
Accepted: July 10, 2015
Published: July 10, 2015

DOI: 10.1021/acsami.5b04522
ACS Appl. Mater. Interfaces 2015, 7, 16760−16766

the water then 900 mg of hexadecylamine (HDA) (Sigma-Aldrich) and 100 mg of copper chloride ($CuCl_2 \cdot 2H_2O$)(Sigma-Aldrich) were added and stirred for 30 min at 1000 rpm. The solution would have turned a homogeneous sky blue color, then 500 mg of D-glucose (α or β) (Merck) was added to it, the stirring speed was reduced to 400 rpm and the reaction was allowed to run for 6 h, then stopped. After the addition of glucose the solution changed color from pale brown to dark brown. The reaction solution was removed from the oil bath and allowed to cool for 10 min after which it was centrifuged at 6500 rpm for 5 min. The Cu NWs were collected at the bottom of the tubes as a neat pellet, which can be easily recovered by carefully decanting the supernatant and gently rinsing the pellet with Mili-Q water a few times.

Cu NWs Ink Formulation. After careful rheology studies it has been found that for every 1 g (wet pellet weight) of Cu NWs, 9.468 mg of HPC is needed to well suspend them. The ink was diluted with Mili-Q water to make a 2.2 mL final ink solution.

Characterization. High-resolution images of the Cu NWs were captured using the FEI Nova NanoSEM 450 FESEM, and the FEI Tecnai T20 TEM. The viscosity measurements were done using a HAAKE Modular Advanced Rheometer System.

RESULTS AND DISCUSSIONS

The drawable electronic inks from high aspect ratio (~1000) copper nanowires (CuNWs) were synthesized by following the recent report with slight modifications.[36] We also thoroughly investigate the rheology properties of the ink to enable us to carefully tailor the ink specifications according to the end applications. The as synthesized Cu NWs have a reddish brown color Figure 1a, are 25−35 nm in diameter Figure 1b and 50−60 μm long Figure 1c. We demonstrated high-performance bending and strain sensors from 2 vol % or 18.28 wt % CuNWs, which is far lower than the spherical nanoparticle inks with typical 60 wt % loading.[20] Our CuNWs inks could be delivered by a ballpoint pen or paintbrush onto paper, PET, and latex rubber substrates, allowing facile patterning of complex design such as the Sydney Opera House. Compared to previous successes in electronics on paper[20,36,37] and PET[5,11,38,39] as flexible, PDMS,[40−42] and Ecoflex[43,44] as stretchable substrates, our CuNWs-based method represents a single, low-cost yet efficient strategy to draw electronics on all these substrates.

The extremely high aspect ratio of the Cu NWs causes them to have a tendency for entanglement and clump formation making it difficult to be used in any ink formulation. To make the Cu NWs into a usable ink, a single polymer additive hydroxypropyl cellulose (HPC) was used. The Cu NWs immediately untangle and form a more homogeneous and well dispersed suspension as soon as the HPC is added. This polymer was chosen as it plays multiple roles of Cu NWs dispersing agent, as a viscosity modifier and also helps to bind the ink to the substrate. The HPC concentration has been carefully controlled so as to not adversely affect the ink's overall electrical conductivity. From the rheology characterization, it has been found that for every 1 g (wet pellet weight) of Cu NWs, 9.5 mg of HPC was required to just suspend them and make an ink that can continuously flow through the ball point without clogging or forming breaks in the ink trace. Increasing the concentration of HPC makes the ink flow smoother but at the expense of a huge loss in electrical conductivity due to cabling effect on the NWs. Hereafter, this ratio of Cu NWs:HPC has been maintained throughout the experiments.

The key requirements in electronic ink are an optimum shear viscosity for smooth ink delivery to the substrate while maintaining trace conductivity. To find this optimum viscosity

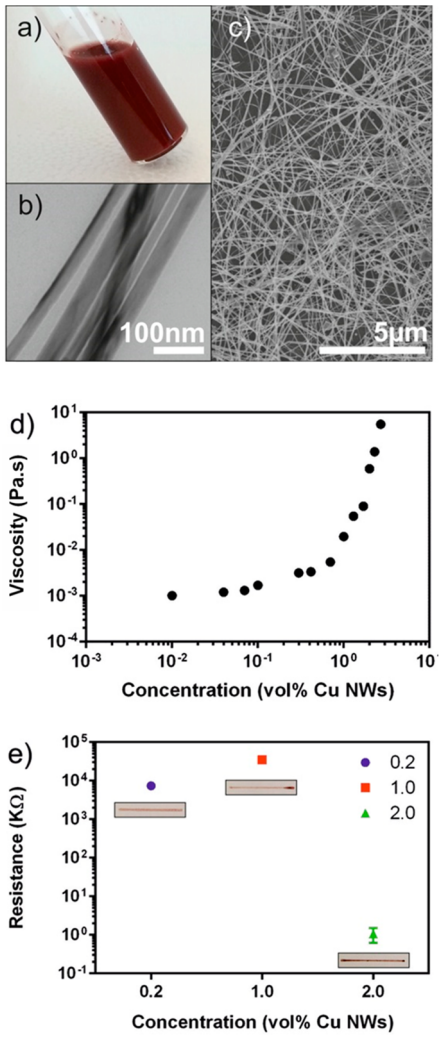

Figure 1. (a) Optical image of Cu NWs ink, (b) TEM image showing diameter, (c) SEM image showing percolation network, (d) Cu NWs concentration vs shear viscosity at 80/s shear rate, and (e) Cu NWs concentration vs resistance at 3 concentrations obtained from shear viscosity chart; 0.2, 1, 2 vol %. Insets show optical image.

we thoroughly investigated the effect of increasing Cu NWs concentration on the ink trace clarity and conductivity. The shear viscosity versus Cu NWs concentration as shown in Figure 1d was measured from an ultralow concentration of 0.01−2.7 vol %, at which the solution was found to have sludge like consistency. This was done in order to have a complete concentration chart of the ink to aid in selecting the concentration best suitable for our application. As drawing will involve various shear rates depending on the strokes and the swiftness of the human hand. It is expected that small strokes will exert low to medium shear rates, and long strokes will exert high shear rates. From our experiments, we estimated that a normal slow writing speed exerts a shear velocity of 1.43 mm/s, and the gap between the ball and the sleeve of the nib is approximately 15 μm from the SEM images. Therefore, assuming the above values, we can estimate the theoretical value of the shear rate from eq 1 to be 95.2/s, which agrees well with our experimental shear rate of 80/s.

$$\dot{\gamma} = \frac{v}{h} \quad (1)$$

DOI: 10.1021/acsami.5b04522
ACS Appl. Mater. Interfaces 2015, 7, 16760−16766

where $\dot{\gamma}$ is the shear rate, υ the shear velocity and h the separation between the two surfaces; in this case the gap between the ball and the sleeve of the nib.

To find the most suitable concentration, one point each from the lower, middle and high concentration ranges were chosen. The aim of testing these different concentrations was to be able to draw a trace which is the thinnest and simultaneously had the highest conductivity. Ink traces were drawn using those concentrations and the resistances were measured, shown in Figure 1e. The low 0.2 vol %, mid 1 vol %, and high 2 vol % concentrations had viscosities of 0.003, 0.02, and 0.6 Pa·s, respectively. The low viscosity/concentration ink had a high ink flow resulting in a substantial efflux of Cu NWs. But the drawback here was that the trace does not hold form and spread on the substrate, resulting in the Cu NWs being spread out on a large area. Hence, due to low concentration of Cu NWs/ink trace area, we had low conductivity. The 0.2 vol % had lowest concentration, hence the highest ink flow among the group, resulting in a wide ink trace but also a high resistance at 7.4 MΩ. On increasing the concentration to 1 vol %, we saw an improvement and the trace becomes thinner. However, owing to the higher viscosity the ink flow was reduced resulting in an even lower Cu NWs/ink trace area and therefore the highest resistance of the group at 32.5 MΩ. The 2 vol % has the highest viscosity hence it has a thin ink trace. The high concentration also makes for high amount of Cu NWs delivery. Therefore, here the constraint of having a thin trace along with a high Cu NWs/ink trace area is achieved. So, this concentration with the best conductivity at 0.85 KΩ was chosen as the concentration for the rest of the experiments.

Our formulated CuNWs inks could be delivered by ballpoint pens and paintbrush uniformly without any observable broken traces. We first tested the feasibility of drawing on paper electronics. Figure 2a is a representative image of a ballpoint pen refill filled with 200 μL of Cu NWs ink and it was used to draw ink traces on four substrates with different surface morphologies: (1) tracing paper, (2) coated photo paper, (3) 100 GSM paper, and (4) PET sheet. Draw-on electronics not only requires a drawable ink but also a drawable substrate. Therefore, it is equally necessary to know about the substrate's surface properties and morphology. The tracing paper surface is rough because of the commercial chemical treatment but still has a continuous surfaces showing no distinct cellulose fibers protruded. Hence, the Cu NWs owing to their ultralong length are able to drape over the peaks and valleys in the surface giving a conductive percolation network with a resistance value of 26.5 kΩ, Supporting Information Figure S1. The 100 GSM paper has the highest resistance among all the ink traces, 3.4 MΩ. This is because of the extremely large cellulose fibers compared to Cu NWs, which are not at all closely packed causing only a few Cu NWs to be able to sustain a very sparse percolation network, Supporting Information Figure S2. The coated photo paper is very absorbent and also very smooth compared to the uncoated based papers allowing for a percolation network to be formed easily (Supporting Information Figure S3) and also resulting in the lowest resistance of 6.6 kΩ for all the traces on the different papers. The coated photo paper looks smooth to the naked eye, but under microscopy inspection reveals a very rough particulate based coated surface. This kind of modified surface is specifically designed to absorb the ink droplet to the maximum extent. A conductive trace of ~500 μm could be drawn on coated photo paper as shown by the brick red color of the copper nanowires (Figure 2b) with a roller ball of 800 μm (Figure 2c). The SEM image in Figure 2d casts a closer look at the ball-point nib. Figure 2e demonstrates the versatility of the ink as it is applied onto a sheet of tracing paper as an elaborate conductive pattern depicting the Sydney Opera House, Supporting Information Figure S9. The glowing LED proves the conductivity of the pattern.

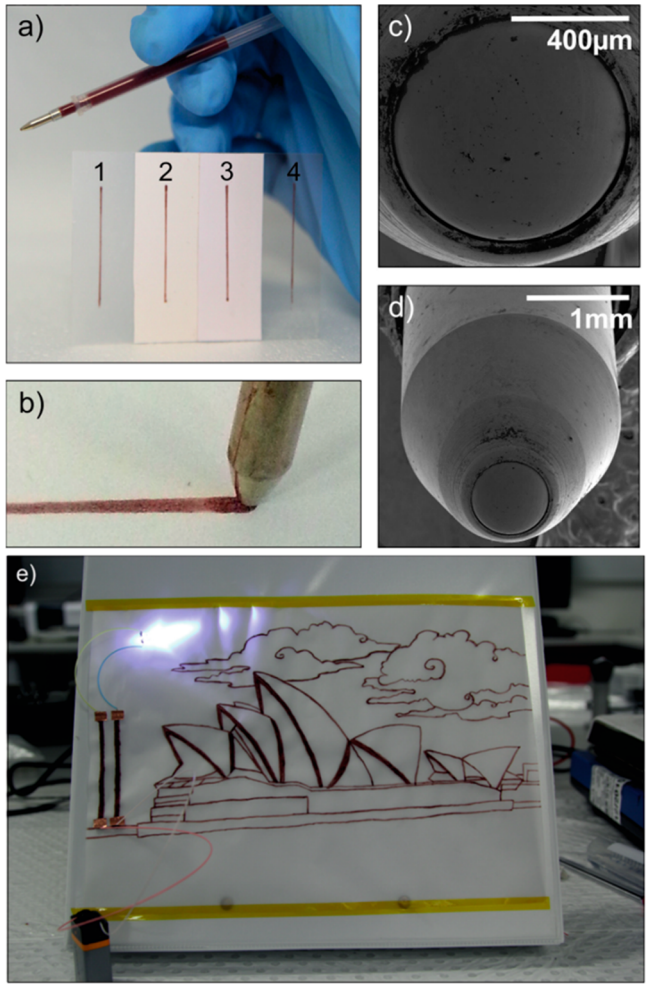

Figure 2. (a) Cu NWs in ballpoint refill in the background, and ink traces on different substrates. (b) Image showing ink trace being drawn by the ballpoint pen on coated photo paper. (c) SEM image showing dimension of the ball. (d) SEM image showing side-view of the ballpoint nib. (e) Painted image of Sydney Opera House, using ink applied by a paintbrush.

To demonstrate the functionality of the ink a bending sensor was fabricated by drawing an array of linear ink traces on a sheet of coated photo paper using the ballpoint pen approach and later a strain sensor was fabricated on latex using the paintbrush approach. For the bending sensor, a series of bending angle tests were done to determine when and where the device starts to fail, as shown in Figure 3. These include, a dynamic measurement bending cyclic test done to test the durability of the device, and a static measurement test for the resistance changes during simple bending at different angles to test the impact of bending on the device's electrical performance. Figure 3a depicts how the linear array of ink traces, each 20 mm long and 5 mm apart are being bent from a flat state to 50°, 130°, and 180°; the corresponding bending radii being 12.5, 6.2, and 2.4 mm, respectively. In Figure 3b, the bending was done at 50° for 10,000 cycles, while measuring the

DOI: 10.1021/acsami.5b04522
ACS Appl. Mater. Interfaces 2015, 7, 16760−16766

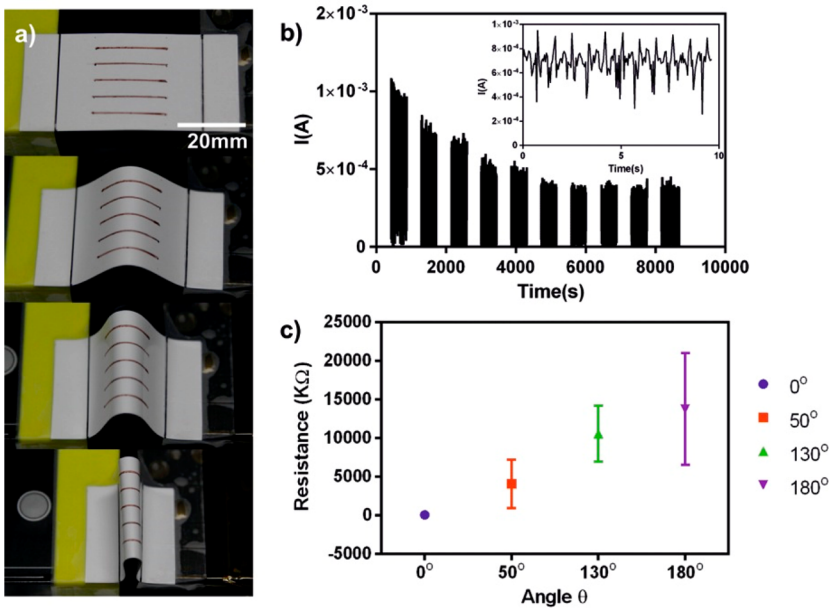

Figure 3. (a) Optical image of Cu NWs conductive ink trace electrode arrays, deposited using a ball-point pen, in flat and bent states, with a bending angles from top to bottom at 0°, 50°, 130°, and 180°. (b) Electrical resistance as a function of bend cycles (10 000) of electrode arrays, at 50° bend. (c) Electrical resistance as a function of bending angle.

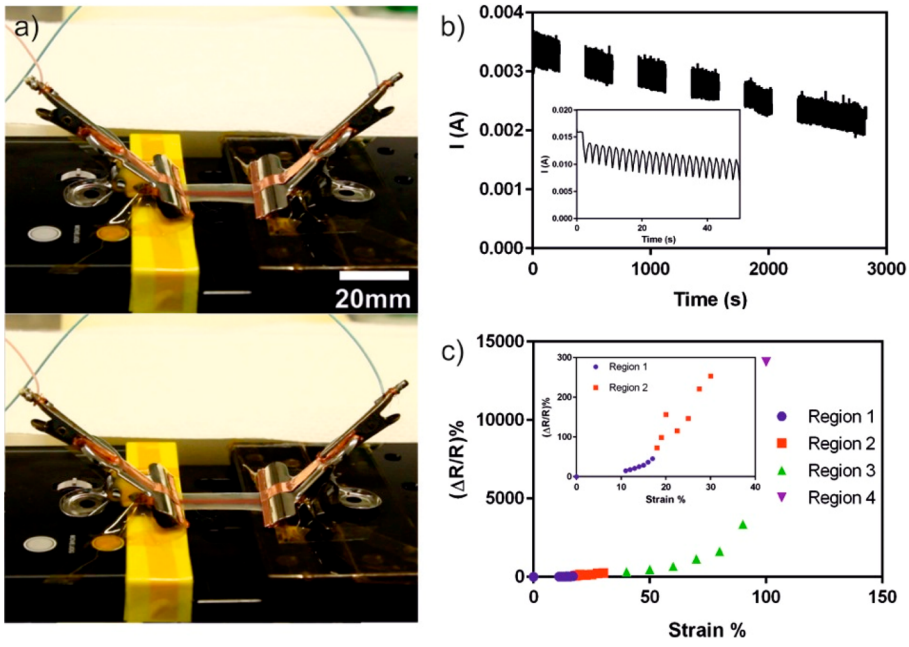

Figure 4. (a) Optical image of Cu NWs conductive ink trace electrode deposited on latex using a paint brush, in relaxed (top) and stretched (bottom) states. (b) Electrical current changes as a function of 10% strain for 6000 cycles, inset 23 cycles at 50% strain. (c) Sensitivity of the strain sensor demonstrated from 0% to 100% strain, inset 0−30% strain.

dynamic current changes. As is evident, the current flow starts to fall from its initial value ∼1 mA until 5000 cycles after which it stabilizes at ∼0.5 mA. The inset Figure 3b, shows the last 10 s of the 5000 cycling tests. Here the baseline stays at ∼0.75 mA, but when the bend occurs, it shoots up to ∼0.9 mA. Furthermore, although the peak in current flow remains fairly constant but there are also intermittent sharp valleys just before or after the peaks along with much noise in the baseline. This may be attributed to the triboelectric effect due to the interaction between the Cu NWs and the rough coated paper surface which maybe generating additional signals apart from the current changes due to bending. The effect of the degree of bending on the device is studied by simply bending the device at 0°, 50°, 130° and 180° and measuring the static resistance, Figure 3(c). We can see that at the resistance is about 200−300 Ω in the absence of bending, but rises quite rapidly to ∼4, ∼9, and ∼14 KΩ for the bending of 50°, 130°, and 180°, respectively. This shows that although the device is sensitive to changes in bending angle, it is also increasingly less reliable at severe bending. Supporting Information Figure S3 depicts a pristine ink trace ∼400 μm wide having an intact percolation network, whereas in Supporting Information Figure S4 which is

DOI: 10.1021/acsami.5b04522
ACS Appl. Mater. Interfaces 2015, 7, 16760−16766

slightly magnified to show serious crack formation after 3000 bending cycles. Both images have been taken from the middle region of the ink trace, the place which is supposed to undergo maximum bending. Even though the NWs are very long, they are not able to sustain a percolation network over the crack that is almost 3−5 μm wide when the paper substrate is flat. This is a failure on the part of the rigid coating on the paper surface, which when in the bent state forms a crack much wider than the length of the Cu NWs themselves, resulting in a ruptured percolation network. During bending the convex surface of the substrate undergoes extensional stress, whereas the concave side experiences compressional stress. In case of smooth substrates such as PET or PDMS, the NWs coating on the convex side will experience NWs breakage and some delamination due to stretching during bending, and also increase in the tightness of contact between NWs. This often results in rise of conductivity during bending. But with severe bending, upon returning to the flat state buckles and waves remain on the NWs coating. The NWs coating is not extensively damaged because of their ability to reversibly slide on a smooth substrate.[45] The present substrate has a rough surface, along with severe crack formations. Reversible sliding of NWs networks is highly unlikely here, which is observed as an obvious fall in the current carrying capacity with increasing bending cycles. This clearly shows that paper although may be able a good substrate for printable and hence "use and throw" electronics, circuits etc., but it may not suitable for human motion sensing applications.

To further test the applicability of the Cu NWs conductive ink in stretchable sensors, a latex strip as a trace 20 mm long and 3 mm wide was drawn using a paint brush. Liquid latex was cast onto a silicon wafer to get a very smooth surfaced latex rubber sheet on which the ink could be easily delivered. Figure 4a depicts the Cu NWs−latex strain sensor in relaxed and stretched states. The cyclic strain tests, Figure 4b are much more stable in terms of current changes and noise compared to the earlier tests, although there is still a weakening trend in current intensity. This is stable until 6000 cycles at least. To measure the sensitivity of the sensor the resistance changes have been plotted against the strain, and the plot shows three distinct sensitivity regimes, Figure 4c. The first regime has a gauge factor of 2.35 in the strain range from 0% to 17%, the second at 13.17 from 18% to 30% Figure 4c inset, and the third at 54.38 from 40% to 90%. It is rare for a single device to have three distinct and also high gauge factors along a large strain range. The first regime shows that the sensor is able to pick up strains with a resolution of 1% strain difference. The medium strain range from 18 to 30% also shows good linearity like the 11−17% range. The 40−90% range has a few outliers but like the previous two ranges has good linearity and high sensitivity. The device shows signs of failing, with aggressive crack formations on the Cu NWs film at 100% strain and the device fails, that is, does not read anymore at 110%. The three trends in the sensitivity curve can be explained on the basis of the increase in the resistivity of the filler material; Cu NWs, the sensing element. This occurs due to the reduction in concentration of the Cu NWs in an area, as a result of being spread out on a larger surface area formed with increasing strain. A more resistive sensing element gives rise to a higher gauge factor.[40] Therefore, when the Cu NWs percolation network goes through three levels of resistivity depending on the strain, we witness three different gauge factors with each one being higher than the previous one. This shows that depending on the sensitivity and the strain range desired, a very accurate strain sensor can be designed simply by varying the concentration of Cu NWs ink and painting it on a rubber substrate.

If we compare the two ink delivery approaches, we will find that the problems that are faced with ball-point pen approach can be overcome with the paintbrush approach. The ball-point pen could not work on the latex substrate because it is not absorbent like paper, hence it was difficult to deposit a sufficient quantity of Cu NWs in the same spot on latex, as was achieved on paper earlier. On paper, retracing the earlier ink mark results in a more connected percolation network, as the ink is absorbed by the paper. But in case of the latex surface, once a trace has been drawn it cannot be retraced as it erodes the percolation network formed by a previous trace. PET sheets also display similar problems because of the surface properties. A critical difference between substrates used for commercial printing and the substrates used in this work, are that for printing the substrate; usually paper, is hydrophobic but it is made super absorbent by inducing surface roughness and using chemical absorbent agents. For such a substrate most printing presses use a hydrocarbon solvent based low surface tension ink, so the ink is absorbed where it comes in contact on the substrate. This results in minimal ink spreading, high ink loading in a small area, as a result high resolution and visual clarity.[46] But an aqueous ink, such as our ink does not absorb well and forms beads. This was overcome by using HPC in our ink which not only lowers the surface tension and reduce beading, but also helps the ink to bind on the paper. Surface roughness is essential for ink absorption, but detrimental for NWs reversible sliding. Now the latex surface is smooth and good for NWs sliding but it is not hydrophilic. Ideally the surface would be made hydrophilic by plasma cleaning but this cannot be done as it induces more cross-linking on the latex surface and cause brittleness and easy tearing of the plasma exposed surface when stretched. The PET surface on the other hand can be oxygen plasma treated to increase the hydrophilic nature and it does not crack like latex. This difficulty with latex was again overcome because of the HPC additive in our ink. This versatile ink even though being aqueous, can be applied to any kind of substrate regardless of the surface properties. When this ink is used on a hydrophilic PET sheet using the ballpoint pen approach the ink runs and does not hold form, and additionally the line could not be retraced to increase Cu NWs concentration. This hurdle was overcome with the paintbrush approach and it was used to paint a trace on an oxygen plasma cleaned PET sheet (and used as a bending sensor (Supporting Information Figures S5−S8), as well as an untreated latex sheet (to retain its smooth surface and stretchability). Recent works show that this approach can actually manipulate even microliter volumes of liquid.[47] As this approach does not erode the previous trace so it is possible to retrace the conductive patterns. In our work, we have also used the conductive ink to actually paint a complex pattern of the Sydney Opera House, Figure 2e and Supporting Information Figure S9, and the conductivity of this pattern is demonstrated by a glowing LED on the painting.

CONCLUSION

In conclusion, we showed that the roller-ball ink delivery approach is well suited for porous, not too rough, absorbent substrates like paper, that is, surfaces for which the ball-point pen has been designed. For smooth but comparatively soft

DOI: 10.1021/acsami.5b04522
ACS Appl. Mater. Interfaces 2015, 7, 16760−16766

substrates like PDMS and latex rubber, the paintbrush approach is a better option. It is noteworthy that the way in which a NP-based ink trace forms a percolation network is very different to the way a NW-based ink trace does; hence, these unique problems. Nonetheless, we have demonstrated that even a hard to use material like Cu NWs can be tailored to be made into a conductive ink with a variety of applications. It is also demonstrated in this work that due to the use of high aspect ratio NWs instead of NPs, we are able to deliver a conductive trace onto a nonuniform substrate, such as coated paper, and even paint a conductive pattern of the Sydney Opera House. These drawable Cu NWs traces exhibited reasonably high stability under ambient conditions (Supporting Information Figures S10 and S11). The use of Cu NWs is highly economical in terms of the conductive filler loading in the ink and the cost of copper itself as compared to other metal NPs, CNT, and graphene-based inks. The demonstrated e-ink, devices, and facile device fabrication methods push the field one step closer to truly creating cheap and highly reliable skin-like devices[18,48] "on the fly"

■ ASSOCIATED CONTENT

Supporting Information

SEM characterization of ink traces on paper, bending tests of ink trace on PET sheet, image of a painting of the Sydney Opera House using Cu NWs ink. The Supporting Information is available free of charge on the ACS Publications website at DOI: 10.1021/acsami.5b04522.

■ AUTHOR INFORMATION

Corresponding Author

*E-mail: wenlong.cheng@monash.edu.

Author Contributions

The manuscript was written by N.N.J and W.C. All authors have given approval to the final version of the manuscript.

Notes

The authors declare no competing financial interest.

■ ACKNOWLEDGMENTS

This work is financially supported by Australia Discovery Projects DP140100052 and DP150103750. The authors thank the Monash Center for Electron Microscopy facilities (MCEM) for the generous use of the FEI Nova NanoSEM 450 FESEM, FEI Tecnai T20 TEM. We also acknowledge the use of the research facilities at the Melbourne Centre for Nanofabrication. N.N.J. also thanks Monash University for the graduate student scholarship (MGS) and the Victorian government for the Victorian International Research Scholarship (VIRS). The authors also acknowledge the help of Amarin G. McDonnell with the viscosity measurements and Chen-Fang Weng with the image processing softwares.

■ ABBREVIATIONS

HDA = hexadecylamine
HPC = hydroxypropyl cellulose
CuNWs = copper nanowires
PET = polyethylene terephthalate
SERS = surface enhanced Raman scattering

■ REFERENCES

(1) Guo, H.; Lin, N.; Chen, Y.; Wang, Z.; Xie, Q.; Zheng, T.; Gao, N.; Li, S.; Kang, J.; Cai, D.; Peng, D. L. Copper Nanowires as Fully Transparent Conductive Electrodes. *Sci. Rep.* **2013**, *3*, 2323−2331.

(2) Lee, J.; Lee, P.; Lee, H.; Lee, D.; Lee, S. S.; Ko, S. H. Very Long Ag Nanowire Synthesis and its Application in a Highly Transparent, Conductive and Flexible Metal Electrode Touch Panel. *Nanoscale* **2012**, *4*, 6408−6414.

(3) Zeng, X. Y.; Zhang, Q. K.; Yu, R. M.; Lu, C. Z. A New Transparent Conductor: Silver Nanowire Film Buried at the Surface of a Transparent Polymer. *Adv. Mater.* **2010**, *22*, 4484−4488.

(4) Rathmell, A. R.; Nguyen, M.; Chi, M.; Wiley, B. J. Synthesis of Oxidation-Resistant Cupronickel Nanowires for Transparent Conducting Nanowire Networks. *Nano Lett.* **2012**, *12*, 3193−3199.

(5) Hu, M.; Gao, J.; Dong, Y.; Li, K.; Shan, G.; Yang, S.; Li, R. K. Flexible Transparent PES/Silver Nanowires/PET Sandwich-Structured Film for High-Efficiency Electromagnetic Interference Shielding. *Langmuir* **2012**, *28*, 7101−7106.

(6) Hu, L.; Kim, H. S.; Lee, J.-y.; Peumans, P.; Cui, Y. Scalable Coating and Properties of Transparent, Flexible, Silver Nanowire Electrodes. *ACS Nano* **2010**, *4*, 2955−2963.

(7) Genovese, M. P.; Lightcap, I. V.; Kamat, P. V. Sun-believable solar paint. A Transformative One-Step Approach for Designing Nanocrystalline Solar Cells. *ACS Nano* **2012**, *6*, 865−872.

(8) Krantz, J.; Richter, M.; Spallek, S.; Spiecker, E.; Brabec, C. J. Solution-Processed Metallic Nanowire Electrodes as Indium Tin Oxide Replacement for Thin-Film Solar Cells. *Adv. Funct. Mater.* **2011**, *21*, 4784−4787.

(9) Lee, J.; Lee, I.; Kim, T. S.; Lee, J. Y. Efficient Welding of Silver Nanowire Networks Without Post-Processing. *Small* **2013**, *9*, 2887−2894.

(10) Xu, F.; Zhu, Y. Highly Conductive and Stretchable Silver Nanowire Conductors. *Adv. Mater.* **2012**, *24*, 5117−5122.

(11) Shen, W.; Zhang, X.; Huang, Q.; Xu, Q.; Song, W. Preparation of Solid Silver Nanoparticles for Inkjet Printed Flexible Electronics with High Conductivity. *Nanoscale* **2014**, *6*, 1622−1628.

(12) Gysling, H. J. Nanoinks in inkjet metallization — Evolution of Simple Additive-Type Metal Patterning. *Curr. Opin. Colloid Interface Sci.* **2014**, *19*, 155−162.

(13) Lawrie, K.; Mills, A.; Hazafy, D. Simple Inkjet-Printed, UV-Activated Oxygen Indicator. *Sens. Actuators, B* **2013**, *176*, 1154−1159.

(14) Layani, M.; Grouchko, M.; Shemesh, S.; Magdassi, S. Conductive Patterns on Plastic Substrates by Sequential Inkjet Printing of Silver Nanoparticles and Electrolyte Sintering Solutions. *J. Mater. Chem.* **2012**, *22*, 14349−14352.

(15) Kim, J.; Kang, J.; Jeong, U.; Kim, H.; Lee, H. Catalytic, Conductive, and Transparent Platinum Nanofiber Webs For FTO-Free Dye-Sensitized Solar Cells. *ACS Appl. Mater. Interfaces* **2013**, *5*, 3176−3181.

(16) Wu, H.; Kong, D.; Ruan, Z.; Hsu, P. C.; Wang, S.; Yu, Z.; Carney, T. J.; Hu, L.; Fan, S.; Cui, Y. A Transparent Electrode based on a Metal Nanotrough Network. *Nat. Nanotechnol.* **2013**, *8*, 421−425.

(17) Wu, H.; Hu, L.; Rowell, M. W.; Kong, D.; Cha, J. J.; McDonough, J. R.; Zhu, J.; Yang, Y.; McGehee, M. D.; Cui, Y. Electrospun Metal Nanofiber Webs as High-Performance Transparent Electrode. *Nano Lett.* **2010**, *10*, 4242−4248.

(18) Gong, S.; Schwalb, W.; Wang, Y.; Chen, Y.; Tang, Y.; Si, J.; Shirinzadeh, B.; Cheng, W. A Wearable and Highly Sensitive Pressure Sensor with Ultrathin Gold Nanowires. *Nat. Commun.* **2014**, *5*, 3132−3140.

(19) Zu, M.; Li, Q.; Wang, G.; Byun, J.-H.; Chou, T.-W. Carbon Nanotube Fiber Based Stretchable Conductor. *Adv. Funct. Mater.* **2013**, *23*, 789−793.

(20) Russo, A.; Ahn, B. Y.; Adams, J. J.; Duoss, E. B.; Bernhard, J. T.; Lewis, J. A. Pen-on-Paper Flexible Electronics. *Adv. Mater.* **2011**, *23*, 3426−3430.

(21) Li, W.; Li, W.; Wei, J.; Tan, J.; Chen, M. Preparation of Conductive Cu Patterns by Directly Writing using Nano-Cu ink. *Mater. Chem. Phys.* **2014**, *146*, 82−87.

DOI: 10.1021/acsami.5b04522
ACS Appl. Mater. Interfaces 2015, 7, 16760−16766

(22) Jia, H.; Wang, J.; Zhang, X.; Wang, Y. Pen-Writing Polypyrrole Arrays on Paper for Versatile Cheap Sensors. *ACS Macro Lett.* **2014**, *3*, 86−90.
(23) Bandodkar, A. J.; Jia, W.; Ramirez, J.; Wang, J. Biocompatible Enzymatic Roller Pens for Direct Writing of Biocatalytic Materials: "Do-it-Yourself" Electrochemical Biosensors. *Adv. Healthcare Mater.* **2015**, *4*, 1215−1224.
(24) Polavarapu, L.; Porta, A. L.; Novikov, S. M.; Coronado-Puchau, M.; Liz-Marzan, L. M. Pen-on-Paper Approach Toward the Design of Universal Surface Enhanced Raman Scattering Substrates. *Small* **2014**, *10*, 3065−3071.
(25) Xu, L. Y.; Yang, G. Y.; Jing, H. Y.; Wei, J.; Han, Y. D. Ag-graphene Hybrid Conductive Ink for Writing Electronics. *Nanotechnology* **2014**, *25*, 55201−55210.
(26) Kurra, N.; Kulkarni, G. U. Pencil-on-Paper: Electronic Devices. *Lab Chip* **2013**, *13*, 2866−2873.
(27) Lin, C. W.; Zhao, Z.; Kim, J.; Huang, J. Pencil Drawn Strain Gauges and Chemiresistors on Paper. *Sci. Rep.* **2014**, *4*, 3812−3818.
(28) Yao, B.; Yuan, L.; Xiao, X.; Zhang, J.; Qi, Y.; Zhou, J.; Zhou, J.; Hu, B.; Chen, W. Paper-Based Solid-State Supercapacitors with Pencil-Drawing Graphite/Polyaniline Networks Hybrid Electrodes. *Nano Energy* **2013**, *2*, 1071−1078.
(29) Kamyshny, A.; Magdassi, S. Conductive Nanomaterials for Printed Electronics. *Small* **2014**, *10*, 3515−3535.
(30) Schirmer, N. C.; Kullmann, C.; Schmid, M. S.; Burg, B. R.; Schwamb, T.; Poulikakos, D. On Ejecting Colloids against Capillarity from Sub-Micrometer Openings: On-Demand Dielectrophoretic Nanoprinting. *Adv. Mater.* **2010**, *22*, 4701−4705.
(31) Shin, K. Y.; Hong, J. Y.; Jang, J. Micropatterning of Graphene Sheets by Inkjet Printing and its Wideband Dipole-Antenna Application. *Adv. Mater.* **2011**, *23*, 2113−2118.
(32) Chen, P.; Chen, H.; Qiu, J.; Zhou, C. Inkjet Printing of Single-Walled Carbon Nanotube/RuO2 Nanowire Supercapacitors on Cloth Fabrics and Flexible Substrates. *Nano Res.* **2010**, *3*, 594−603.
(33) Song, J. W.; Kim, J.; Yoon, Y. H.; Choi, B. S.; Kim, J. H.; Han, C. S. Inkjet Printing of Single-Walled Carbon Nanotubes and Electrical Characterization of the Line Pattern. *Nanotechnology* **2008**, *19*, 95702−95708.
(34) Tang, Y.; Gong, S.; Chen, Y.; Yap, L. W.; Cheng, W. Manufacturable Conducting Rubber Ambers and Stretchable Conductors from Copper Nanowire Aerogel Monoliths. *ACS Nano* **2014**, *8*, 5707−5714.
(35) Tang, Y.; Yeo, K. L.; Chen, Y.; Yap, L. W.; Xiong, W.; Cheng, W. Ultralow-Density Copper Nanowire Aerogel Monoliths with Tunable Mechanical and Electrical Properties. *J. Mater. Chem. A* **2013**, *1*, 6723−6726.
(36) Zhou, Y.; Fuentes-Hernandez, C.; Khan, T. M.; Liu, J. C.; Hsu, J.; Shim, J. W.; Dindar, A.; Youngblood, J. P.; Moon, R. J.; Kippelen, B. Recyclable Organic Solar Cells on Cellulose Nanocrystal Substrates. *Sci. Rep.* **2013**, *3*, 1536−1541.
(37) Zhu, H.; Fang, Z.; Preston, C.; Li, Y.; Hu, L. Transparent Paper: Fabrications, Properties, and Device Applications. *Energy Environ. Sci.* **2014**, *7*, 269−287.
(38) Kim, J.; Yun, J. M.; Jung, J.; Song, H.; Kim, J. B.; Ihee, H. Anti-Counterfeit Nanoscale Fingerprints based on Randomly Distributed Nanowires. *Nanotechnology* **2014**, *25*, 155303−155310.
(39) Chung, W. H.; Hwang, H. J.; Lee, S. H.; Kim, H. S. In Situ Monitoring of a Flash Light Sintering Process using Silver Nano-Ink for Producing Flexible Electronics. *Nanotechnology* **2013**, *24*, 35202−35210.
(40) Amjadi, M.; Pichitpajongkit, A.; Lee, S.; Ryu, S.; Park, I. Highly Stretchable and Sensitive Strain Sensor based on Silver Nanowire-Elastomer Nanocomposite. *ACS Nano* **2014**, *8*, 5154−5163.
(41) Gutruf, P.; M Shah, C.; Walia, S.; Nili, H.; S Zoolfakar, A.; Karnutsch, C.; Kalantar-zadeh, K.; Sriram, S.; Bhaskaran, M. Transparent Functional Oxide Stretchable Electronics: Micro-Tectonics Enabled High Strain Electrodes. *NPG Asia Mater.* **2013**, *5*, e62−e69.
(42) Wang, X.; Gu, Y.; Xiong, Z.; Cui, Z.; Zhang, T. Silk-Molded Flexible, Ultrasensitive, and Highly Stable Electronic Skin for Monitoring Human Physiological Signals. *Adv. Mater.* **2014**, *26*, 1336−1342.
(43) Fan, J. A.; Yeo, W. H.; Su, Y.; Hattori, Y.; Lee, W.; Jung, S. Y.; Zhang, Y.; Liu, Z.; Cheng, H.; Falgout, L.; Bajema, M.; Coleman, T.; Gregoire, D.; Larsen, R. J.; Huang, Y.; Rogers, J. A. Fractal Design Concepts for Stretchable Electronics. *Nat. Commun.* **2014**, *5*, 3266−3274.
(44) Yao, S.; Zhu, Y. Wearable Multifunctional Sensors using Printed Stretchable Conductors made of Silver Nanowires. *Nanoscale* **2014**, *6*, 2345−2352.
(45) Wu, J.; Zang, J.; Rathmell, A. R.; Zhao, X.; Wiley, B. J. Reversible Sliding in Networks of Nanowires. *Nano Lett.* **2013**, *13*, 2381−2386.
(46) Wu, J.; Liu, L.; Jiang, B.; Hu, Z.; Wang, X. Q.; Huang, Y. D.; Lin, D. R.; Zhang, Q. H. A Coating of Silane Modified Silica Nanoparticles on PET Substrate Film for Inkjet Printing. *Appl. Surf. Sci.* **2012**, *258*, 5131−5134.
(47) Wang, Q.; Su, B.; Liu, H.; Jiang, L. Chinese Brushes: Controllable Liquid Transfer in Ratchet Conical Hairs. *Adv. Mater.* **2014**, *26*, 4889−4894.
(48) Kim, D.-H.; Lu, N.; Ma, R.; Kim, Y.-S.; Kim, R.-H.; Wang, S.; Wu, J.; Won, S. M.; Tao, H.; Islam, A.; Yu, K. J.; Kim, T.-i.; Chowdhury, R.; Ying, M.; Xu, L.; Li, M.; Chung, H.-J.; Keum, H.; McCormick, M.; Liu, P.; Zhang, Y.-W.; Omenetto, F. G.; Huang, Y.; Coleman, T.; Rogers, J. A. Epidermal Electronics. *Science* **2011**, *333*, 838−843.
(49) Jin, M.; He, G.; Zhang, H.; Zeng, J.; Xie, Z.; Xia, Y. Shape-Controlled Synthesis of Copper Nanocrystals in an Aqueous Solution with Glucose as a Reducing Agent and Hexadecylamine as a Capping Agent. *Angew. Chem., Int. Ed.* **2011**, *50*, 10560−10564.

DOI: 10.1021/acsami.5b04522
ACS Appl. Mater. Interfaces 2015, 7, 16760−16766